

# On Stabilization of Gas Puff Implosion: Experiment and Simulation

Rina B. Baksht, Anatoliy V. Fedunin, Aleksey Yu. Labetsky, Alexander G. Russkikh, Alexander V. Shishlov, Oleg V. Diyankov, Igor V. Glazyrin, and Serge V. Koshelev

**Abstract**—A double gas puff was used to study the mitigation of the magneto-Rayleigh–Taylor (RT) instabilities for long implosion times (up to 250 ns). The experiments have been performed on the inductive storage GIT-4 (1.7 MA, 120 ns) generator. Current division between the outer and inner shells was controlled using magnetron-discharge preionization. The implosion of the a double gas puff, with the improved preionization, results in the formation of a uniform plasma column. The results of two-dimensional (2-D) radiation-magnetohydrodynamic simulations support the experimental results: a double gas puff implosion mitigates the RT instabilities, leading to the development of only small-amplitude waves. The 2-D simulation allowed us to explain the halo effect seen in the experiments: the use of the low hybrid conductivity in the calculation demonstrated the existence of the high density plasma core surrounded by a low density plasma halo.

**Index Terms**—Plasma radiation sources, plasma stability.

## I. INTRODUCTION

IN plasma radiation sources (PRS), Z-pinch loads are imploded to generate large amounts of soft X-rays with 1–10 keV photon energies [1], [2]. However, the radiative powers and sometimes energies of the PRS measured in the experiments is less than is predicted by one-dimensional (1-D) simulations. The magneto-Rayleigh–Taylor (RT) instability is one of the main reasons for the decrease in the efficiency of the energy transfer from a driver to the PRS. The RT instability can result in the plasma shell being disrupted, especially for large diameter loads [3], [4]. A structured load is known to mitigate the RT instability. In particular, a multilayer (double or more) gas puff can be used to improve the dynamics of an imploded load.

A double gas puff was first realized by Sincerny *et al.* [5] for a Kr radiation source on a capacitor bank with 1-MA current. The authors [5] demonstrated the efficiency of the double gas puff in comparison with a large diameter gas puff: there was a 1.6-fold increase in the maximum power of the total radiation. Later the authors [6], [7] carried out experiments with double and three layer gas puffs on a capacitor bank with a 0.3-MA current, using Ne, Ar, and Kr gases. In these experiments a 1.5–2-fold increase in the total radiation energy was observed.

Manuscript received August 10, 1997; revised February 10, 1998. This work was supported by ISTC Project 525 and CRDF Grant 1-180.

R. B. Baksht, A. V. Fedunin, A. Yu. Labetsky, A. G. Russkikh, and A. V. Shishlov are with the Institute of High Current Electronics, Tomsk, 634055, Russia.

O. V. Diyankov, I. V. Glazyrin, and S. V. Koshelev are with the Russian Federal Nuclear Center-VNIITF, Snezhinsk, Chelyabinsk Region, Russia.

Publisher Item Identifier S 0093-3813(98)07003-9.

Theoretical papers on the suppression of the RT instability with multishell gas puffs appeared simultaneously with the experimental work mentioned above. Theoretical analysis [4] and simulations [8] demonstrated the high efficiency of a structured load and showed that for certain conditions it is possible to mitigate the RT instability and to obtain higher values of the K-shell yield. Workers [9] have tried to obtain the required parameters, which are derived from the theoretical analysis, with argon double gas puffs. The experiments [9] demonstrated that the problem of current division between the gas puff layers is a crucial obstacle to achieving successful multishell gas-puff implosions. It was shown that in the real experimental conditions a gas-puff is not a homogeneous, highly conductive plasma cylinder during the first nanoseconds when a high voltage is applied to the anode-cathode gap.

A gas puff can be considered as a gas shell with several current channels (streamers) during the initiation phase. As a result, a highly conductive skin layer is not produced in a gas shell, and part of the applied current can flow through the inner shell, i.e., the current divides between the shells. It is clear that this results in magnetic field penetration inside the outer shell and the deterioration of the implosion dynamics. Magnetron preionization of the outer shell [10] prevented the current division. In this paper, we will describe the Ar double gas puff experiments with both spark and magnetron preionization of the outer shell. Furthermore, we will compare the experimental data with the results of two-dimensional (2-D) magnetohydrodynamic (MHD) calculations. The GIT-4 experimental arrangement is described in Section II, and the experimental results are discussed in Section III. Section IV contains the 2-D MHD calculations, and we draw our conclusion in Section V.

## II. EXPERIMENTAL ARRANGEMENTS

Experiments were carried out on the GIT-4 inductive storage generator [11] with 1.7-MA load current and 120-ns plasma open switch (POS) opening time. The GIT-4 upstream inductance  $L_{up}$  is equal to 220 nH; the downstream inductance  $L_d$  is 70 nH. The value  $L_d$  is determined by the 30-cm distance between the POS and the load. Owing to the large distance between the POS and the load [12], the POS resistance rises rapidly. The measurements [13] showed that the POS resistance rises up to 1.2–1.4 Ohm in 60–80 ns, and then remains almost constant during the Z-pinch implosion. Typical waveforms of the upstream and downstream currents and a

TABLE I  
SUMMARY OF DATA CONCERNING DIVISION OF CURRENT BETWEEN THE OUTER AND INNER SHELLS OF A DOUBLE GAS PUFF [10]

	Probability that current will flow through outer shell only, %	Probability that current will divide between outer and inner shells, %	Number of shots
without preionisation	30	70	15
spark preionisation on anode	36	64	11
spark preionisation on cathode	100	0	10
Planar magnetron discharge	100	0	5

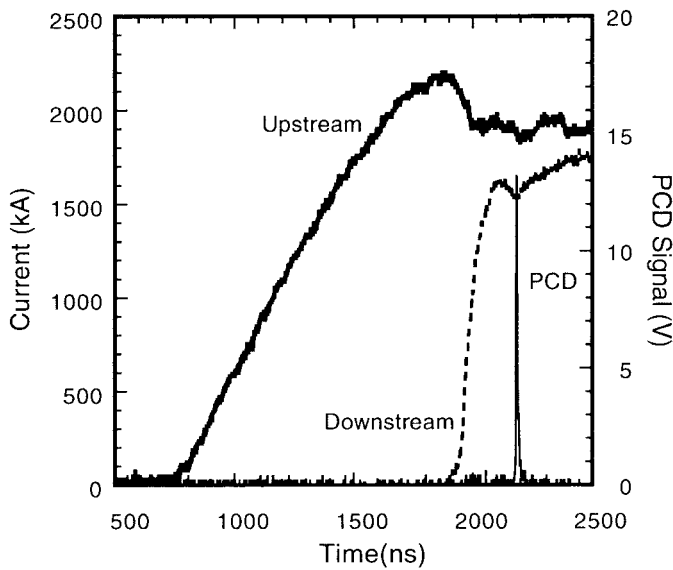


Fig. 1. Typical currents and K-shell PCD waveforms for the Ar double gas implosion [shot #398; mass of the 1.4-cm inner shell is  $80 \mu\text{g}/\text{cm}$ ; mass of the 3-cm outer shell is  $35 \text{ (g/cm)}$ ].

PCD signal are shown in Fig. 1 for an Ar double gas puff implosion.

All the experiments were performed with the preionization of an outer shell. However, only the magnetron preionization ensures the absence of the inner shell current for any electrode configuration. This is confirmed by the data from the tests of different preionization systems (Table I). These tests were performed on the IMRI-4 facility and was described in detail in [10].

The design of the GIT-4 nozzle and preionization assembly is shown in Fig. 2. The nozzle assembly was located on the anode of the downstream section. Three spark gaps were located at the distance of 25 mm from the exit of the nozzle. A small capacitor bank (4 kV,  $0.5 \mu\text{F}$ ) was triggered  $8 \mu\text{s}$  prior to the onset of the load current. A small magnet coil was located near the outer nozzle which produced a pulsed 0.03-T magnetic field in the outer shell. The copper plug was used to reduce the magnetic field in the inner shell area. The design

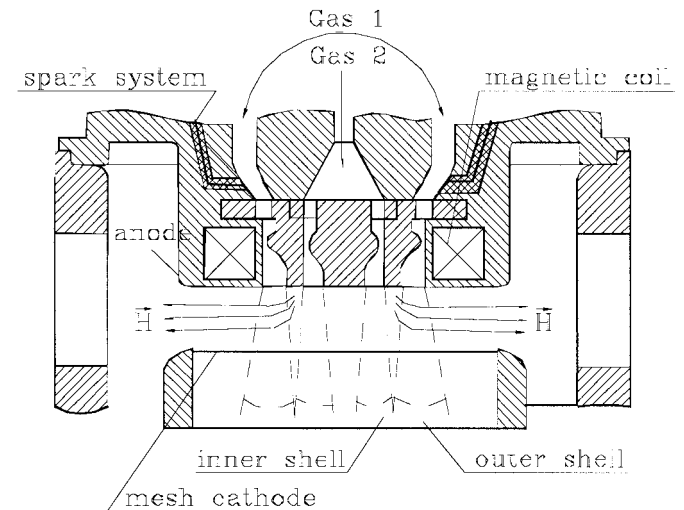


Fig. 2. Design of the nozzles and the preionization assembly for the GIT-4 facility.

of the valve allowed for independent plenum pressures in the inner and outer shell.

The GIT-4 generator was fired  $450 \mu\text{s}$  after the onset of gas flow. The plenum pressure for the outer shell was 0.3 atm ( $m \approx 30 \mu\text{g}/\text{cm}$ ); the plenum pressure for the inner shell was varied between  $1 \div 2.5 \text{ atm}$  ( $m \approx 60 \div 180 \mu\text{g}/\text{cm}$ ). The radius of the inner shell is 1.4 cm, the outer one is 3 cm; the anode-cathode gap is 2 cm. In the experiments with a single gas puff, the gas was fed only in the inner shell with the radius of 1.4 cm.

The gas puff implosion is monitored with various diagnostics. The radial and axial dynamics of the implosion are measured with a streak camera as described in [9]. A double-film-stack, time-integrated pinhole camera was fielded. The filter was  $2 \mu\text{m}$  Kimfol plus  $0.2 \mu\text{m}$  aluminum (the transmission threshold is approximately 0.8 keV). Two films were placed inside the pinhole camera, one behind the other. The first film absorbs photons with energies below 3 keV, so one can obtain the argon K-shell image on the second film. The K-shell spectra emission (3–4 keV) from the pinched plasma is measured with a time integrated mica spectrograph. The X-ray yields and powers are measured using both a

TABLE II  
SUMMARY OF DOUBLE GAS PUFF EXPERIMENTS WITH SPARK AND MAGNETRON PREIONIZATIONS

Shot #	Pressure in the inner shell plenum, atm	Mass in the inner shell*, $\mu\text{g}/\text{cm}$	MD preionisation	P_k, GW	E_k, J	Precursor pulse
403	1	60	No*	25.8	442	No
385	1.5	80	No	39.8	616	No
386	1.5	80	No	26.6	399	No
394	1.5	80	No	33	460	Yes
396	1.5	80	Yes	58.7	444	No
397	1.5	80	Yes	37	359	No
398	1.5	80	Yes	51	403	No
399	1.5	80	No	24.2	374	Yes
400	1.5	80	No	40.7	402	Yes
404	2	110	No	29	311	Yes
405	2	110	Yes	52	343	No
406	2.5	160	Yes	21	128	No
387	2.5	160	No	16.5	173	No

\* The quantity of mass in the inner shell is the imploded mass per unit length based on the measured currents and implosion times for the single gas puffs.

\* «No» means that there is only the spark preionisation; «yes» means that there is the spark preionisation plus B-field.

filtered, diamond photo conducting detector (PCD) [14] and an aluminum cathode X-ray diode (XRD).

### III. EXPERIMENTAL RESULTS

The measured K-shell yields and powers versus the inner-shell plenum pressure are plotted in Fig. 3 for double- and single-shell gas puff implosions. It can be seen that the double shell gas puff configuration produces an increase in the K-shell yield.

A summary of the measured parameters for the spark and the magnetron discharge (MD) preionizations are shown in Table II. The spark system was used on all shots. A large scatter in measured K-shell powers and energies is observed for double gas puff with only the spark preionization. The scatter reduced when the magnetic field was employed in conjunction with the sparks. In the later case, the spark was used to reduce the statistical time lag of the breakdown. We note that there is approximately 1 kV potential difference between the anode and the cathode during 1.3  $\mu\text{s}$  conduction phase of the plasma opening switch. We believe that this assists in the preionization prior to the onset of downstream current.

In the last column of Table II some results of the XRD measurements are shown. A precursor pulse (see Fig. 4) in

the soft X-ray radiation was measured in most of the shots with the spark preionization only, and it was absent in the shots with the MD preionization.

The main result of the use of the magnetron discharge for preionization is the production of more stable plasma columns in the stagnation phase. Comparison between a single-shell gas puff implosion (shot #378) and a double-shell gas puff implosion with the MD (shot #398) demonstrates that the stagnation phase of the double-shell gas puff implosion is the more uniform (see Fig. 5 and Table III). Bright spots are observed in the pinhole picture corresponding to the shot #378, but they are absent in the pinhole picture corresponding to the shot #398. The bright spots have higher temperatures but lower densities (shot #378) than the stable plasma columns. The final plasma column of the double-shell gas puff implosion (shot #398) is like the structure observed in Sandia wire array experiments [15], [16]: a stable core with high efficiency of K-shell radiation gives the clear cut pinhole picture for 3 keV photons. The core which has a 1 mm full width at half maximum (FWHM) diameter is surrounded by a 3.4 mm FWHM halo (Fig. 6). The temperatures in the halo are low as it can only be seen on the 0.8 keV pinhole picture. Instabilities are visible on the outside of the halo plasma. However, the

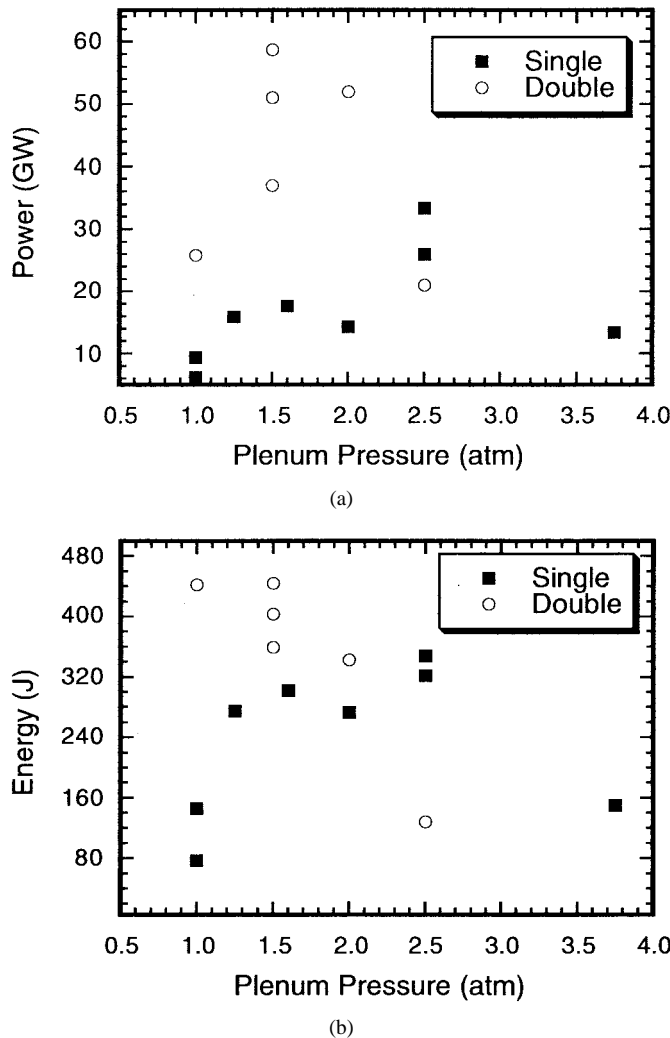


Fig. 3. (a) The measured K-shell power and (b) K-Shell yield versus the inner gas puff plenum pressure for double and single gas puffs.

amplitudes are small and they do not extend into the hot plasma region.

#### IV. TWO- DIMENSIONAL MHD NUMERICAL ANALYSIS

Two-dimensional MHD simulations have been carried out to explain the following phenomena: 1) the uniform final plasma column and 2) the halo formation.

The MAG code [17] was used for the simulation. The system of equations used in the MAG code is determined by the Braginskii [18] model for the one-temperature case (electron temperature is equal to ion temperature). The average charge states of the ions were taken from the Ermakov-Kalitkin tables [19]. Radiation transfer was not accounted in the calculation; radiation losses were determined from the results of 1-D simulations using the ERA code [20] which took into account radiation transport and ionization dynamics.

The magnetic field at the boundary of the mesh was determined by solving a circuit equation. Since preionization was used, the case of current flowing in the inner shell was not considered. The preionization of the outer shell was treated

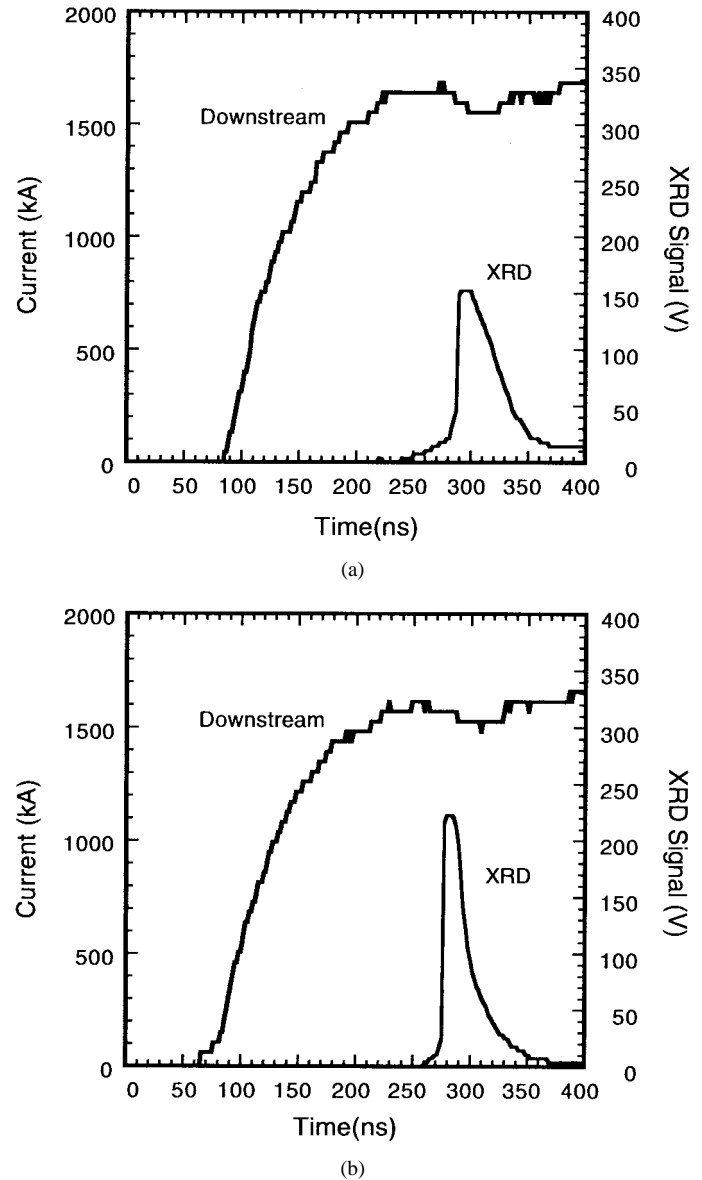


Fig. 4. (a) Soft XRD and downstream current waveforms for double gas puff with spark preionization and (b) MD preionization. There is a precursor for the case (a). The XRD was filtered by  $2 \mu$  of Kimfol and  $0.2 \mu$  of aluminum.

by supposing that at the start of the simulation the outer shell had an average charge state equal to one. Then, in the process of the simulation, the current was distributed in accordance with the magnetic field diffusion. It is important to note that in the diffusion of magnetic field, the Hall term and the term connected with spontaneous magnetic field formation were not included.

Various gas puff configurations were considered in the simulations (single-shell and double-shell gas puffs with different mass ratios of the inner to the outer shell). To seed the RT instability development, an initial random density perturbation was used. The numerical mesh was 60 cells along the radius and 200 cells along the  $z$ -axis, so we could treat the development of the instabilities with a mode number up to 40.

In order to analyze the RT instability development, the density profile along the  $z$ -axis was extended into Fourier

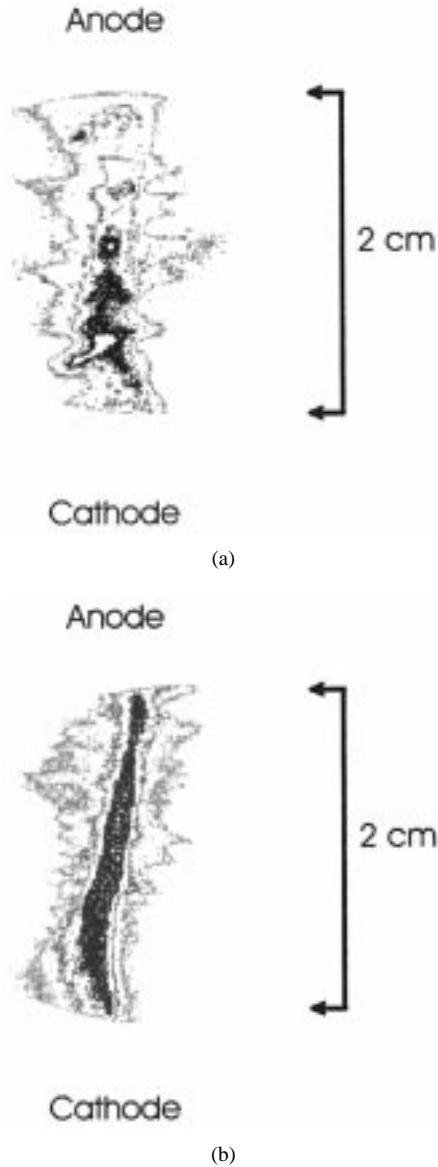


Fig. 5. (a) The pinhole pictures for double gas puff with spark preionization and (b) MD preionization. The bright spots are absent when the MD preionization is used.

series

$$\rho = \sum_{\kappa=0}^{\kappa=K} \rho_{\kappa} \exp^{ikz} \quad (1)$$

where  $\rho_{\kappa}$  is the density,  $k = n\pi/l$ ,  $k$  is the wave number, and  $l$  is the gas puff length. Large  $k$  corresponds to the evolution of small scale instabilities; small  $k$  corresponds to the evolution of long wavelength instabilities. In the linear approximation, the instability amplitude  $A$  could be expressed as

$$A = \exp^{\int \gamma dt}$$

where  $\gamma$  is the instability increment.

During the implosion of the outer shell instabilities grow, with the shorter wavelength instabilities growing more rapidly as determined by (1) until the outer shell strikes the inner one. The nature of the subsequent instability behavior depends on the ratio of the shell masses. In the case when the outer shell

TABLE III  
SUMMARY OF DATA FOR A SINGLE GAS PUFF AND A DOUBLE GAS PUFF

	Sh.No.378	Sh.No.398
$m_{in}$ , $\mu\text{g}/\text{cm}$	180	80
$r_{in}$ , cm	1.4	1.4
$m_{out}$ , $\mu\text{g}/\text{cm}$	0	30
$r_{out}$ , cm	0	3
P, GW	33	51
T, keV	1	0.65
$n_i$ , $\text{cm}^{-3}$	$0.8 \cdot 10^{19}$	$5 \cdot 10^{19}$

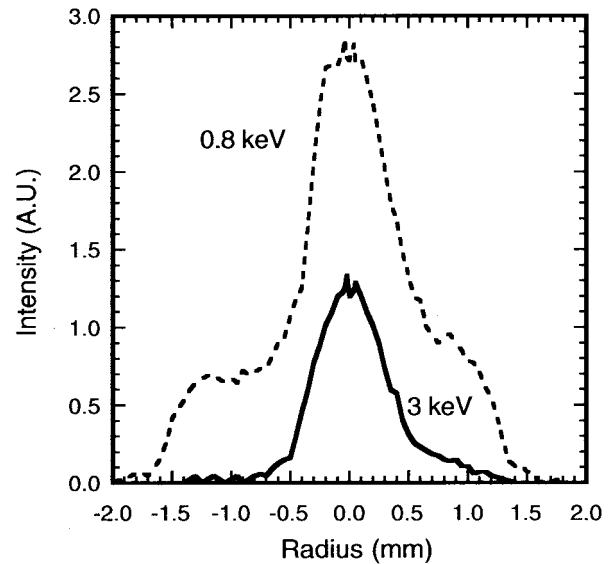


Fig. 6. Radial profile measured by the pinhole camera image showing the core and halo spatial distribution.

is heavier than the inner one, the instabilities can still grow rapidly which can lead to the formation of the hot spots. In the case when inner shell is more massive, the amplitudes of the instabilities are suppressed during the collision of outer and inner shells. As a result, a low density halo with small scale nonuniformity could be observed around the uniform plasma column.

The values of harmonic amplitudes versus time are shown in Figs. 7–9. Two gas puff configurations were considered: 1) double-shell gas puff with the outer shell being three times lighter than the inner one (80  $\mu\text{g}/\text{cm}$ , the inner shell mass and 30  $\mu\text{g}/\text{cm}$ , the outer shell mass); 2) double-shell gas puff with reversed mass ratio (30  $\mu\text{g}/\text{cm}$ , the inner shell mass and 80  $\mu\text{g}/\text{cm}$ , the outer shell mass). In Fig. 7, we denote the curves by the mass of the inner shell.

In Fig. 7 the time dependence of the wave amplitude of the sausage mode of instability is shown for two cases described above. It is seen that the mode with  $k = \pi/l$  grows more intensively in the case of the light inner shell. As a result, the hot spots form in the final stage of the implosion. In the case when the inner shell is heavier than the outer one, the modes

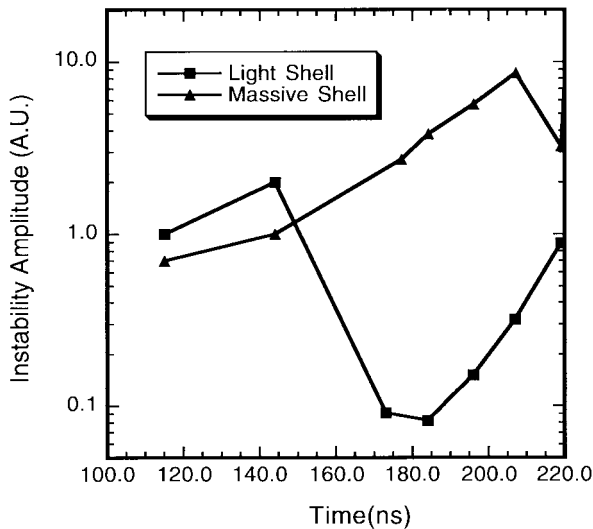


Fig. 7. Simulated amplitude of the sausage mode with  $k = \pi/l$  of the instability versus time for two variants of the double gas puff: (a) double gas puff with the outer shell being three times lighter than the inner one; (b) double gas puff with reversed ratio of the shell masses. The dips of the curves coincide with the moment of the collision of the outer and inner shells. Zero time coincides with the onset of the load current.

with small  $k$  is suppressed during the impact that leads to the quasi 1-D implosion.

We think that the mechanism of stabilization is similar to that described in [21]. When the bubbles in the outer shell, which appear as a result of  $k = \pi/l$  instability development, reach the inner shell of the gas puff, hot plasma regions are produced (the temperature in these regions is approximately two times greater than in the surrounding plasma). Thus, two shock waves begin to propagate from this region along the boundary in  $z$  direction, heating plasma at the boundary of the inner shell. The temperature increase of the plasma leads to the rise in electric conductivity so that the gradient of the magnetic field at the boundary increases as well. When the lagging part of the outer plasma shell reaches the inner shell, the pressure at the boundary between the plasma and magnetic field equalizes along the  $z$ -axis and then the magnetic field continues compressing the combined and more uniform plasma shell in the radial direction. The “snowplow” mechanism of the instability suppression described in [4] looks similar to this one. For the massive outer shell, harmonics with  $k = \pi/l$  are more dangerous (see Fig. 7) because the pressure of the light inner shell is not large enough, and the “snowplow” mechanism does not work.

The instability with  $k = 2\pi/l$  grows slowly in the case of the light outer shell (see Fig. 8). Since the amplitudes of the higher harmonics are close to each other, the average amplitude of harmonics from  $k = 4\pi/l$  up to  $k = 20\pi/l$  was calculated (see Fig. 9). The average amplitude of harmonics grows rapidly in the case of the light outer shell. It leads to the generation of the small-scale wave observed in the experiments at the boundary between the plasma and the magnetic field.

The simulation for a single gas puff shows that the maximum temperature in the hot spot formed by the development of the instability during the implosion of a single gas puff is higher than the maximum temperature in the plasma column

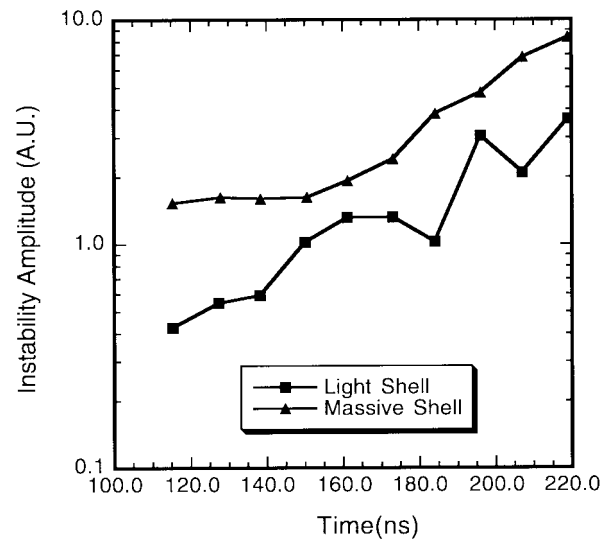


Fig. 8. Simulated amplitude of the  $k = 2\pi/l$  mode of the instability versus time for two variants of the double gas puff: (a) double gas puff with the outer shell being three times lighter than the inner one; (b) double gas puff with reversed ratio of the shell masses. Zero time coincides with the onset of the load current.

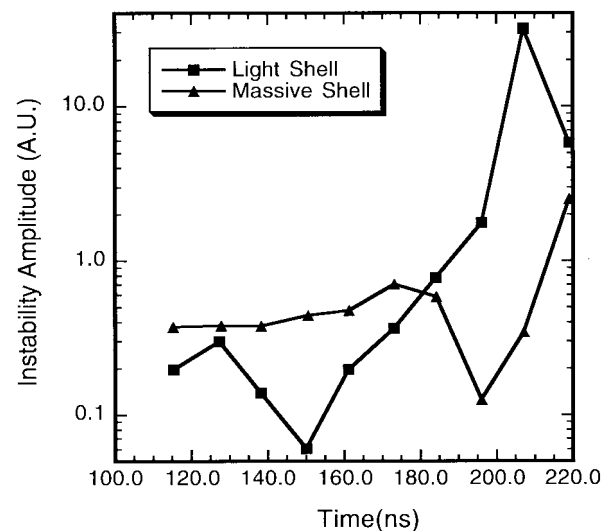


Fig. 9. Simulated average amplitude of the highest modes of the instability versus time for two variants: (a) double gas puff with the outer shell being three times lighter than the inner one; (b) double gas puff with reversed ratio of the shell masses. Zero time coincides with the onset of the load current.

resulting from the uniform compression of a double gas puff. This fact is well supported by the experimental data (see Table III). However, the mean specific energy of the stable plasma column is higher, and thus the K-shell yield increases. It is also confirmed by the experimental data.

The halo phenomenon observed in the experiments could be explained if the force of magnetic pressure acting on the inner layer of the plasma shell exceeds the force acting on the outer layer. As a result, the plasma density near the axis is greater than that in the surrounding area. The use of Spitzer conductivity in the simulation gives uniform compression without halo formation. A mechanism that could be responsible for the fast penetration of the magnetic field is anomalous resistivity. We assume that the anomalous resistivity is determined by the low

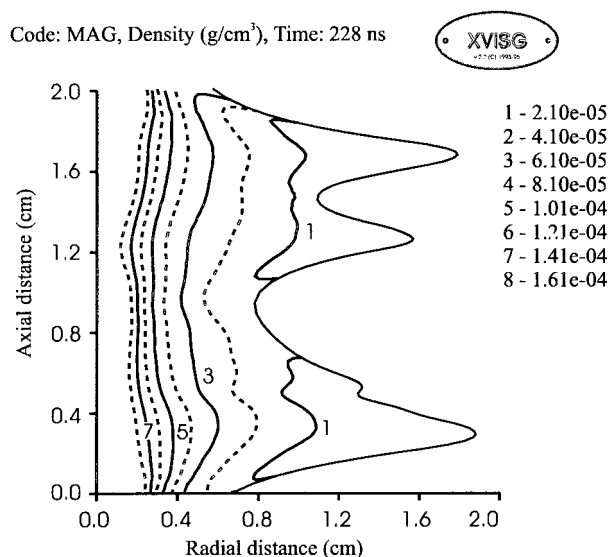


Fig. 10. Calculated density distribution near the time of maximum compression for shot #398. Contours 7 and 8 describe the dense core and contours 1–3 describe the low-density halo.

hybrid instability [20]. Calculated density profiles are shown in Fig. 10. The contours are isodensity with the eight contours covering one decade as a logarithmic sequence. Fig. 10 shows the dense plasma core and perturbed low-density halo. The difference between the experimental image (see Figs. 5 and 6) and the picture obtained in the numerical simulation (see Fig. 10) is connected with the fact that: 1) the pinhole image does not correspond to the density distribution and 2) the resolution of the numerical mesh does not allow us to describe a small-scale instability.

## V. CONCLUSION

Two-dimensional MHD simulations combined with experiments have demonstrated that by using a double-shell gas puff configuration it is possible to achieve the formation of a uniform pinched plasma column without hotspots. Small amplitude instabilities are observed only in the outer halo regions, and they do not extend into the most dense part of the pinched plasma. The mass of the gas puff material radiating in the K-shell energy region from the core region is equal to  $32 \mu\text{g/cm}$  (i.e., 28% of the initial gas puff mass). In order to involve a higher fraction of the mass of a gas puff in the process of radiating K-shell X-ray emissions, the 2-D calculations suggest that it is necessary to improve the implosion quality thereby decreasing the mass in the cool halo. Since gas puff implosions formed by high atomic number materials are known to be more stable, we will study the use of Kr outer shell as one of the ways for further improvement of double-shell gas puff stability.

## REFERENCES

- [1] N. R. Pereira and J. Davis, "X-rays from Z-pinch on relativistic electron-beam generators," *J. Appl. Phys.*, vol. 64, no. 3, pp. R1–R27, Aug. 1988.
- [2] K. G. Whitney, W. Thornhill, J. L. Guiliani, J. Davis, L. A. Miles, E. E. Nolting, V. L. Kenyon, W. A. Spicer, J. A. Draper, C. R. Parsons, P. Dang, R. B. Spielman, T. J. Nash, J. S. McGurn, L. E. Ruggles, C.

- Deeney, R. R. Prasad, and L. Warren, "Optimization of K-shell emission in aluminum Z-pinch implosions: Theory versus Experiment," *Phys. Rev. E*, vol. 50, no. 3, pp. 2166–2174, Aug. 1994.
- [3] D. L. Peterson, R. L. Bowers, J. H. Brownell, A. E. Greene, H. Lee, W. Matuska, "Two-dimensional simulations of foil implosion experiments of the Los Alamos Pegasus bank," in *AIP Conf. Proc.*, vol. 299, pp. 388–395, 1993.
- [4] A. Velikovich and S. Golberg, "Suppression of Rayleigh-Taylor instability by the snowplow mechanism," *Phys. Fluids B*, vol. 5, pp. 1164–1173, May 1993.
- [5] P. Sincerny, S. Wong, and V. Buck, "Pulsed compression with an imploding gas puff," in *Proc. 5th Pulsed Power Conf.*, Arlington, VA, 1985, pp. 701–703.
- [6] R. B. Baksht, A. V. Luchinskii, and A. V. Fedunin, "Soft X-ray source using a cascaded liner," *Sov. Phys.—Tech. Phys.*, vol. 37, no. 11, pp. 1118–1120, Nov. 1992.
- [7] R. B. Baksht, S. P. Bougaev, I. M. Datsko, A. V. Fedunin, I. A. Schemakin, A. V. Luchinsky, Yu. D. Korolev, V. G. Rabotkin, V. I. Oreshkin, "Implosion of multilayer liners," *AIP Conf. Proc., Proc. 3rd Int. Conf. Dense Z-pinchs*, London, U.K. vol. 299, pp. 365–371, 1993.
- [8] F. L. Cohan, J. Davis, and A. L. Velikovich, "Stability and radiance performance of structured Z-pinch loads imploded on high-current pulsed power generators," *Phys. Plasmas*, vol. 2, no. 7, pp. 2765–2772, July 1995.
- [9] R. B. Baksht, I. M. Datsko, A. F. Fedunin, A. A. Kim, A. Yu. Labetsky, S. V. Loginov, A. V. Shishlov, V. I. Oreshkin, "The Rayleigh–Taylor instabilities and K-radiation yield for imploding gas liners," *Plasma Phys. Rep.*, vol. 21, pp. 907–912, Nov. 1995.
- [10] R. B. Baksht, A. G. Russkikh, and A. A. Chagin, "Study of the effect of preionization on current sharing between sheaths of a double-cascade gas puff," *Plasma Phys. Rep.*, vol. 23, no. 3, pp. 175–182, Mar. 1997.
- [11] S. P. Bugaev, B. M. Kovalchuk, G. A. Mesyats, A. A. Kim, A. N. Batrikov, V. A. Kokshenev, "A Terawatt pulsed power generator with a microsecond plasma open switch," *IEEE Trans. Plasma Sci.*, vol. 18, pp. 115–118, Jan. 1990.
- [12] D. Mosher, S. J. Stephanakis, J. P. Apruzese, D. C. Black, J. R. Boller, R. J. Comisso, M. C. Meyer, G. G. Peterson, B. C. Weber, and F. C. Young, "Radius scaling of X-radiation from gas puff load implosions on an inductive driver," in *Proc. 4th Int. Conf. Dense Z-pinchs*, Vancouver, Canada, vol. 409, pp. 135–140, 1997.
- [13] A. V. Shishlov, "Determination of the effective resistance of a plasma opening switch," *Instrum. Exp. Tech.*, vol. 40, no. 1, pp. 79–81, Jan. 1997.
- [14] R. B. Spielman, "Diamond photo conducting detectors as high power Z-pinch diagnostics," *Rev. Sci. Instrum.*, vol. 63, no. 10, pp. 5056–5067, Nov. 1992.
- [15] T. W. L. Sanford, T. S. Nash, R. C. Mock, R. B. Spielman, J. F. Seamen, J. S. McGurn, D. Jobe, T. L. Gilliland, M. Vargas, K. G. Whitney, W. Thornhill, P. G. Pulsifier, and J. P. Apruzese, "Time dependent electron temperature diagnostics for high-power aluminum Z-pinch plasmas," in *Proc. 11th Amer. Physical Soc. Topical Conf. High Temp. Plasma Diagnostics*, Monterey, CA, 1996.
- [16] T. W. L. Sanford, G. O. Allshouse, T. S. Nash, B. M. Marder, R. C. Mock, R. B. Spielman, J. F. Seamen, J. S. McGurn, D. Jobe, T. L. Gilliland, M. Vargas, J. Hammer, J. DeGroot, J. L. Eddleman, D. D. Peterson, D. Mosher, K. G. Whitney, J. W. Thornhill, P. G. Pulsifier, J. P. Apruzese, and Y. Maron, "Improved symmetry greatly increases X-ray power from wire-array Z-pinchs," *Phys. Rev. Lett.*, vol. 77, no. 25, pp. 5063–5066, Dec. 1996.
- [17] O. V. Diyankov, I. V. Glazyrin, and S. V. Koshelev, "MAG—two-dimensional resistive MHD code using arbitrary moving coordinate system," to be published.
- [18] S. L. Braginskii, "Transport in plasmas," *Review of Plasma Physics*, M. A. Leontovich, Ed. New York: Consultant Bureau, 1965, vol. 1, pp. 205–271.
- [19] V. V. Ermakov and N. N. Kalitkin, "Tables of the electrical conductivity and electron heat conductivity coefficients for the plasma of 11th substances" (in Russian), in *Preprint Appl. Math. Inst.*, 1978.
- [20] I. V. Glazyrin, N. G. Karlykhonov, A. A. Kondratev, V. G. Nikolaev, M. S. Timakova, "One-dimensional modeling of double gas puff implosion with anomalous resistivity consideration," *AIP Conf. Proc., Proc. 3rd Int. Conf. Dense Z-pinchs*, London, U.K., vol. 299, pp. 139–144, 1993.
- [21] I. V. Glazyrin, O. V. Diyankov, N. G. Karlykhanov, S. V. Koshelev, "Numerical modeling of MHD instabilities in Z-pinch hot spot," *Proc. 12th Int. Conf. High-Power Particle Beams*, Prague, Czech Republic, June 10–14, 1996, pp. 717–721.

**Rina B. Baksht** graduated from the Department of Electric Engineering, Tomsk Polytechnic Institute, Russia, in 1960. She received the Kandidat degree in 1968, and the Doctor degree in 1992.

She joined the Institute of High Current Electronics, Tomsk, Russia, in 1977. She is the principal investigator of projects related to the soft X-ray generation, the study of the combined (gas puff on wire) pinch system, the use of inductive storage for plasma and electron beam loads, and hardware design for pulse power generators with currents in the range of 100-600 kA.



**Anatoliy V. Fedunin** was born in 1955. He graduated from the Department of Physics, Tomsk State University, Russia, in 1978.

He worked in the aerospace industry and, in 1985, joined the Institute of High Current Electronics, Tomsk, Russia. Since then, his work has been involved in the design and the development of gas puff for use the X-ray radiation sources.



**Aleksey Yu. Labetsky** was born in 1972. He graduated from the Department of Physics, Tomsk State University, Russia, in 1994. At present he is a postgraduate student of the Department of Physics, Tomsk State University. He is carrying out his Ph.D. work at the Institute of High Current Electronics, where he is engaged in plasma diagnostics.



**Alexander G. Russkikh** was born in 1964. He graduated from the Department of Physics, Tomsk Polytechnic Institute, Russia, in 1987.

He joined the Institute of High Current Electronics, Tomsk, Russia, in 1987. Since then, his work has been involved in the development of gas puff physics. His interests are the preionization and plasma formation in gas puff devices.



**Alexander V. Shishlov** was born in Tomsk, Russia, in 1968. He graduated from the Department of Physics, Tomsk Polytechnic Institute.

He joined the Institute of High Current Electronics, Russian Academy of Sciences, Tomsk, in 1993. His research interests include the experimental study of Z-pinch plasma and plasma diagnostics.

**Oleg V. Diyankov** was born in Russia in August 1958. He received the degree in mathematics in Novosibirsk State University, Russia.

In 1980 he joined the Russian Federal Nuclear Center-VNIITF working on the field of numerical modeling of MHD flows. He lectured also on mathematics at the Chelyabinsk Division of Moscow Engineering Physics Institute.

**Igor V. Glazyrin** was born in Russia on January 1963. He received the degree in theoretical physics in Chelyabinsk State University, Russia.

In 1985 he joined the Russian Federal Nuclear Center-VNIITF working in the field of numerical modeling of MHD flows.

**Serge V. Koshelev** was born in Russia in October 1970. He received the degree in physics in Novosibirsk State University, Russia.

In 1992 he joined the Russian Federal Nuclear Center-VNIITF working in the field of numerical modeling and scientific visualization.